Calculating the 3-dimensional current in the ionosphere and its associated magnetic perturbation

Astrid Maute[1] and Arthur D. Richmond[1]

High Altitude Observatory; National Center for Atmospheric Research, Boulder CO, USA [1].

Background

Ionospheric electric fields and currents are driven by collisional interaction between thermospheric winds and ions, by magnetospherically driven ion convection and field-aligned currents at high latitudes, by gravitational and pressure gradient forces on the ionospheric plasma, and by weak currents from the lower atmosphere.

For simulating the electric field due to these different drivers we assume that the electric potential is nearly constant along geomagnetic field lines, and therefore the electric field variations can be expressed in two dimensions. The current density, however, depends also on the conductivity distribution **σ**, and consequently varies in all three dimensions.

The objective is to determine the 3D current and its associated magnetic perturbation

- **To accurately determine the magnetic perturbation at Low Earth Orbit (LEO) altitudes it is important to consider the 3D current variation.**
- **The 3D current and LEO magnetic perturbation can be used as a diagnostic and can be compared to satellite measurements, e.g., Magsat, Ørsted, CHAMP, Swarm.**
- **It further our understanding of the physical processes especially in the equatorial ionosphere.**
- **A possible application is the assimilation of LEO magnetic perturbations into numerical models.**

3D current model

The formulation to solve for the global ionospheric electric potential Φ and to calculate the ionospheric current **J** is consistent and satisfies

$$\nabla \cdot \boldsymbol{J} = 0 \quad (1)$$

over each element (blue element in Fig. 1). The electric potential is solved for at the center of the element (red big point) and the electric field **E** can be calculated from

$$\boldsymbol{E} = -\nabla\Phi \quad (2)$$

at the blue interface points. The divergence of the wind driven current $\mathbf{J}_w$, the plasma pressure gradient and gravity driven current, $\mathbf{J}_p$ and $\mathbf{J}_g$, respectively, are balanced by the convergence of electric field driven current $\mathbf{J}_E$ and field-aligned current $\mathbf{J}_\parallel$

$$-\nabla \cdot [\boldsymbol{J}_E + \boldsymbol{J}_\parallel] = \nabla \cdot [\boldsymbol{J}_w + \boldsymbol{J}_p + \boldsymbol{J}_g] \quad (3)$$

with

$$\boldsymbol{J}_E = [\sigma_P \boldsymbol{E}_\perp + \sigma_H \boldsymbol{b}_o \times \boldsymbol{E}_\perp] \quad (4)$$

$$\boldsymbol{J}_w = [\sigma_P \boldsymbol{u} \times \boldsymbol{B}_o + \sigma_H \boldsymbol{b}_o (\boldsymbol{u} \times B_o)] \quad (5)$$

$$\boldsymbol{J}_p = -\frac{1}{B_o{}^2} \nabla P \times \boldsymbol{B}_o \quad (6)$$

$$\boldsymbol{J}_g = \frac{n_e m_i}{B_o{}^2} \boldsymbol{g} \times \boldsymbol{B}_o \quad (7)$$

and σ_P and σ_H are the Pedersen and Hall conductivity, respectively, the neutral wind is **u**, $\mathbf{E}_\perp$ is the electric field perpendicular to the geomagnetic main field $\mathbf{B}_o$ with the unit vector $\mathbf{b}_o$. The plasma pressure P is $P = n_e k_B (T_i + T_e)$ with the electron density n_e, the ion and electron temperature T_i and T_e, respectively, and the Boltzmann constant k_B. The gravitational acceleration is **g**, and the ion mass is m_i.

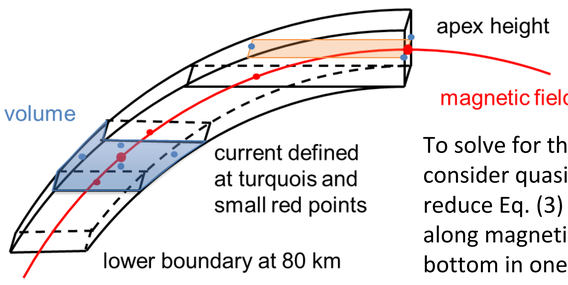

Figure 1: Schematic of discretization along a field line.

To solve for the electric potential we consider quasi steady state and can reduce Eq. (3) to 2D by integrating $\nabla \cdot J_\perp$ along magnetic field lines from the bottom in one hemisphere to the other.

The boundary conditions for the field line integration are the current from the lower atmosphere and at the top of the model the high latitude field aligned current calculated from an empirical ion convection pattern and ionospheric conductivities.

3D current: Once $\mathbf{E}_\perp$ is calculated the current perpendicular to **B** can be determined from Eq. (4)-(7). The current is defined at the interfaces of each element to ensure current continuity. The current density $\mathbf{J}_\parallel$ is determined from the integrated divergence of $\mathbf{J}_\perp$ along a field line.

The electric field **E** can be separated into components associated with each current source $\mathbf{E}=\mathbf{E}_w+\mathbf{E}_p+\mathbf{E}_g$, where each component drives conduction current that closes its source current e.g., $\nabla\cdot(\mathbf{J}_w+\mathbf{J}(\mathbf{E}_w))=0$.

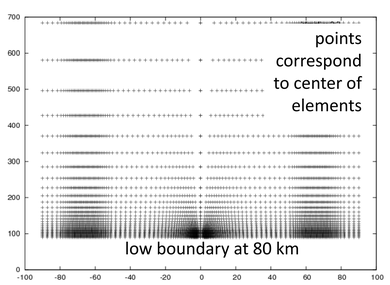

Figure 2: Example of discretization.

The discretization is flexible and to resolve the strong height and/or latitudinal gradients at auroral and equatorial latitudes the resolution is refined in these regions (Figure 2). The vertical resolution is defined by fixed heights corresponding to the apex of low latitude field lines. In the E-region this leads to roughly 1/3 scale height resolution but increasing towards the top of the model.

Is all the current flowing in the E-region?

- Wind driven current $\mathbf{J}_w+\mathbf{J}(E_w)$ (blue line) dominates in the daytime E-region with ~450 to 650 nA/m² in the equatorial ionization anomaly (EIA) region.
- The $\mathbf{J}_w+\mathbf{J}(E_w)$ is the largest current component up to ~200 km in the EIA region.
- In the F-region the wind driven source current $\mathbf{J}_w$ is small, while $\mathbf{J}(E_w)$ is larger ~10nA/m² because of $\mathbf{E}_w$ generated mainly by the E-region dynamo.
- In the F-region $\mathbf{J}_p$ and $\mathbf{J}_g$ are important and the dominant current sources in the EIA region with magnitudes of ~20-30 nA/m² at 15LT and 20 LT.
- The $\mathbf{J}_p$ is westward above the F-region peak and eastward below. $\mathbf{J}_p$ is almost balance but there is a small eastward current $\mathbf{J}(E_p)$ in the E-region.
- The $\mathbf{J}_g$ is eastward and closed through the daytime E-region with a westward current $\mathbf{J}(E_g)$.

To accurately determine the magnetic perturbations at LEO height it is important to take the height variation of the current into account which the 3D model can do.

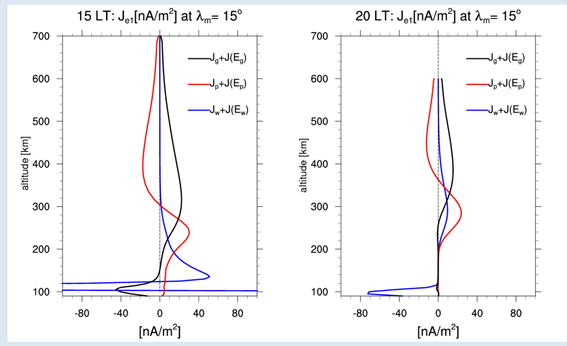

Figure 3: Magnetic eastward current [nA/m²] at magnetic latitude λ_m=15° and magnetic longitude ϕ_m=15° for September solar maximum conditions ($F_{10.7}$=200) at 15 local time (LT) and 20 LT (19UT and 0UT, respectively).

Ionospheric currents and their associated magnetic effects

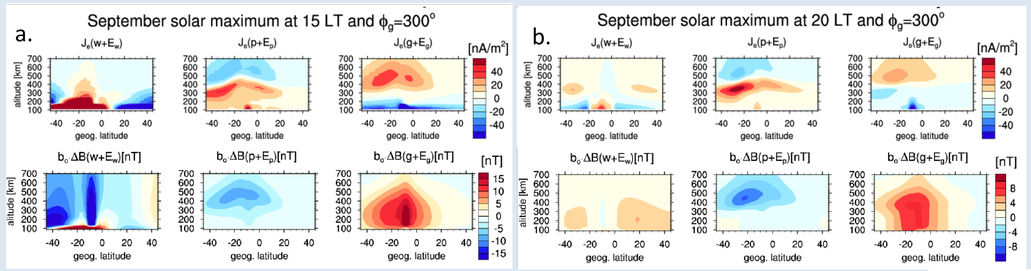

Figure 4: Geographic eastward current [nA/m²] (top panels) and scalar magnetic perturbations [nT] (bottom panels) at λ_g=300° for September ($F_{10.7}$=200) at a. 15 LT (19 UT) and b. 20 LT (0UT) due to J(w,E_w), J(p,E_p), and J(g,E_g).

- The E-region westward return current J(E_g) is up to ~350 nA/m² at the equator, and ~30-60 nA/m² at mid-latitude at 15LT, while ~80 nA/m² at 20 LT. The magnetic signal $b_o\cdot\Delta B(g+E_g)$ is therefore positive and decreases with altitude in the F-region.
- $b_o\cdot\Delta B(p+E_p)$ is negative and reduces the main magnetic field. The E-region eastward current J(E_p) (~70 nA/m² at 15 LT) leads to negative equatorial perturbation.

- At 515 km $b_o\cdot\Delta B$ due to J(w+E_w) is almost of similar magnitude as due to J(p+E_p) and J(g+E_g) at 15 LT and even smaller at 20 LT (Fig. 5).
- The day–night difference in $b_o\cdot\Delta B(g+E_g)$ and $b_o\cdot\Delta B(p+E_p)$ is smaller than in $b_o\cdot\Delta B(w+E_w)$.
- $b_o\cdot\Delta B(g+E_g)$ and $b_o\cdot\Delta B(p+E_p)$ have opposite signs.

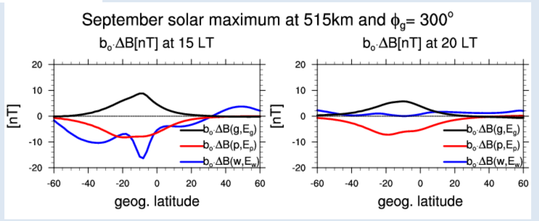

Figure 5: Scalar magnetic perturbations [nT] at 515 km

Comparison of approximated $b_o\cdot\Delta B$ with 3D calculation

- The diamagnetic effect is an approximation of the plasma pressure gradient forcing effect and assumes $\frac{(B_o+\Delta B)^2}{2\mu_o} + P = \text{constant}$.
- Lühr et al. [2003] using CHAMP data quantified the diamagnetic effects with -5 nT in the EIA region based on $\Delta B_{diamag} = -P\frac{\mu_o}{B_o}$ with μ_o the permeability of free space.
- The diagmagnetic effect (Fig.6a top) overestimates the magnetic effect at mid-latitude and underestimates it at low latitude since the influence of J(E_p) is not included.
- The magnetic signal of J(g,E_g) is approximated by $\Delta B_g(h) = \mu_o \int_h^{h_{top}} J_g(h')dh'$
- The approximation ΔB_g (Fig. 6b top) doesn't take into account the westward E-region return current J(E_g) which is especially strong at the magnetic equator.

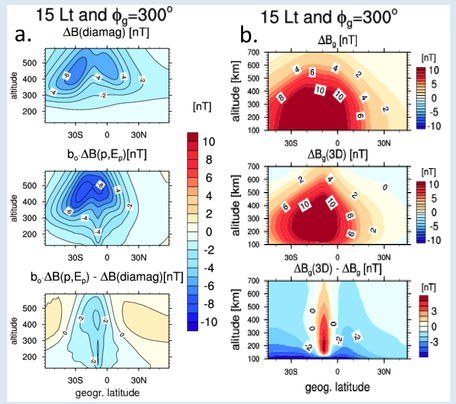

Figure 6: $b_o\cdot\Delta B$ [nT] at 15 LT for September with $F_{10.7}$=200 due to plasma pressure gradient (a) and gravity (b) driven current: approximation (top); using3D current (middle); difference (bottom).

Magnetic effects due to combined gravity and plasma pressure gradient driven current

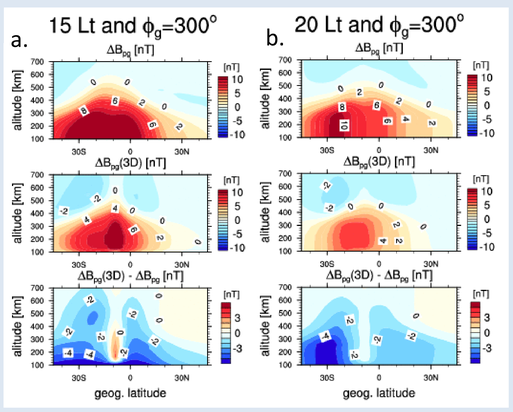

Figure 8: $b_o\cdot\Delta B$ due to J_p+J(E_p) and J_g+J(E_w) for September & $F_{10.7}$=200 for 15 LT (a) and 20 LT (b): approximation (top), using 3D current (middle), difference (bottom).

- Combing the current J(p,g+E_{pg}) reduces in general the magnetic effect in the upper F-region compared to J(p,E_p) or J(g,E_g) alone.
- However, in the lower F-region the magnetic signal varies strongly with altitude.
- The magnetic signal should not be corrected for the diamagnetic effect alone.
- Using the approximations for $b_o\cdot\Delta B(p,g,E_{pg})$ does not reduce the error in the top F-region (Fig. 8 middle & bottom). However, the simulation indicates that in the bottom F-region the error in the approximation is less than the signal itself.
- At LEO height during solar minimum $b_o\cdot\Delta B(p,g+E_{pg})$ is very small (Fig. 9) and can probably be neglected especially at night.
- Even for solar maximum $b_o\cdot\Delta B(p,g+E_{pg})$ is small after 22 LT (Fig. 10).
- Capturing the current sources is important when analyzing satellite data for studying, e.g., the equatorial electrojet, and not removing the effect can lead to bias in, e.g., higher order magnetic field models.

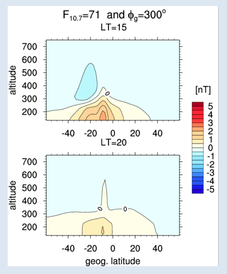

Figure 9: $b_o\cdot\Delta B(p,g+E_{pg})$ at 15 LT and 20 LT for $F_{10.7}$=71.

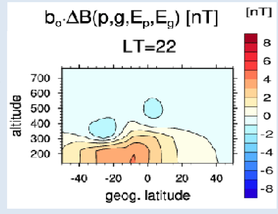

Figure 10: $b_o\cdot\Delta B(p,g+E_{pg})$ at 22 LT for $F_{10.7}$=200.

Reference Lühr, H., M. Rother, S. Maus, W. Mai, and D. Cooke (2003), The diamagnetic effect of the equatorial Appleton anomaly: Its characteristics and impact on geomagnetic field modeling, *Geophys. Res. Letters*, *30*(17).

Acknowledgment A.M. and A.D.R. were supported by NSF grant AGS-1135446. The National Center for Atmospheric Research is sponsored by the National Science Foundation.